ISTITUTO DI ANALISI DEI SISTEMI ED INFORMATICA
CONSIGLIO NAZIONALE DELLE RICERCHE

S. Salinari, A. Bertuzzi, G. Mingrone, E. Capristo, A. Pietrobelli, P. Campioni, A.V. Greco, S.B. Heymsfield

BIOIMPEDANCE ANALYSIS MODEL ACCURATELY PREDICTS LOWER LIMB MUSCLE VOLUME: VALIDATION USING MAGNETIC RESONANCE IMAGING

R. 527 Giugno 2000

Serenella Salinari – Dipartimento di Informatica e Sistemistica, Università di Roma "La Sapienza", via Eudossiana 18, 00184 Roma, Italy. Email : salinari@dis.uniroma1.it.

Alessandro Bertuzzi – Istituto di Analisi dei Sistemi ed Informatica del CNR, viale Manzoni 30 - 00185 Roma, Italy. Email : bertuzzi@iasi.rm.cnr.it.

Geltrude Mingrone, Esmeralda Capristo, Aldo V. Greco – Istituto di Medicina Interna e Geriatria, Università Cattolica del Sacro Cuore, Largo A. Gemelli 8 - 00168 Roma, Italy. Email : gmingrone@unicatt.it.

Angelo Pietrobelli, Steven B. Heymsfield – Obesity Research Center, St. Luke's–Roosevelt Hospital, Columbia University College of Physicians and Surgeons, New York, New York 10025, USA.

Paolo Campioni – Istituto di Radiologia, Università Cattolica del Sacro Cuore, Largo A. Gemelli 8 - 00168 Roma, Italy.

ISSN: 1128–3378

Collana dei Rapporti
dell'Istituto di Analisi dei Sistemi ed Informatica, CNR

viale Manzoni 30, 00185 ROMA, Italy

tel. ++39-06-77161
fax ++39-06-7716461
email: iasi@iasi.rm.cnr.it
URL: http://www.iasi.rm.cnr.it

Abstract

Bioimpedance analysis (BIA) methods are oversimplified in the representation of lower limb geometry and electrical properties. The feasibility of using multiple BIA measurements for quantifying muscle volume and for reconstructing the profile of the muscle cross-sectional area along the lower limb was cross-validated by magnetic resonance (MRI) data. A three dimensional model of the lower limb was assembled by segmentation of magnetic resonance cross-sectional images for adipose tissue, skeletal muscle and bone. An electrical network was then associated with this model. MRI and BIA measurements were made in 6 lean subjects (3 men and 3 women, age 32.2 ± 6.9 years). Assuming 0.85 S/m for the longitudinal conductivity of the muscle, the model predicted in the examined subjects an impedance profile that conformed well to the BIA profile; predicted and measured resistances were similar (261.3±7.7 vs 249±9 Ω). By use of a simpler model, the resistance profile provided muscle area estimates along the lower limb and total leg muscle volume (mean 4,534 cm^3 for men and 4,071 cm^3 for women) with a mean of the absolute value of the relative error of 6.2±3.9% with respect to MRI. Our new BIA approach suggests BIA can reasonably estimate the distribution and volume of muscles in the lower extremities.

Key words: Bioimpedance analysis, body composition, nutritional assessment, magnetic resonance imaging.

1. Introduction

The study of human body composition in health and disease is of increasing interest both in research and clinical practice (11). The availability of advanced techniques, such as computed tomography (CT) and magnetic resonance imaging (MRI), allows precise and reproducible estimates of major tissue and organ compartments (9,12). However, CT and MRI can be performed only in specialized research units, as the availability of gear time is limited, the cost is high and technical expertise is required for image analysis (18).

In the past decade, bioimpedance analysis (BIA) has been advocated as a simple method for the determination of body composition in humans, as it is non invasive, inexpensive and well-suited for epidemiological studies (3). However, current BIA electrical and geometrical models are oversimplified and the results are often inaccurate (3,5). Typically, BIA estimates of total body water (TBW) are based upon equations in which the fat-free compartment is assumed as a cylinder with uniform electrical characteristics and the height of the subject is taken into account in order to adjust for between-individual differences in electrical path length. The conventionally used path length in bioimpedance analysis is arm-to-leg, although the measurement of isolated limb or trunk impedance is now gaining recognition (2,16,17). Recently, a detailed analysis of resistance data of human thigh was reported by Aaron et al. (1) and resistance data from the thigh and calf were analyzed in association with MRI body composition estimates by Fuller et al. (7).

The aim of the present study was to evaluate the feasibility of using multiple BIA measurements for quantifying muscle volume and for reconstructing the profile of the muscle cross-sectional area along the lower limb. Lower limb was selected as the study site because it has a simpler geometry and tissue composition compared to the trunk. Our study was based on a mathematical model that describes the electrical characteristics of the lower limb in lean healthy subjects. The mathematical model utilizes a realistic reconstruction of limb geometry and tissue composition obtained from MRI measurements. The model provides the distribution of electrical potential and the fluxes of current induced in the lower limb by an externally applied current and thus allows for a comparison with BIA measurements at multiple sites along the lower limb. Furthermore, on the basis of the results obtained by the model, a method for reconstructing muscle cross sectional area along the lower limb from BIA data is proposed.

2. Subjects and Methods

Subjects and anthropometry

Six volunteers (3 men and 3 women, age [mean±SD] 32.2 ± 6.9, body mass index $22.4 \pm 1.4\,\mathrm{kg/m^2}$) were enrolled in the study. All subjects were in good health, as assessed by clinical and laboratory examinations, were not taking medications and did not participate in intensive physical activity. The women were studied in the follicular phase of the menstrual cycle. Body weight was measured to the nearest 0.1 kg by a beam scale, and height to the nearest 0.5 cm using a stadiometer (Holatin, Crosswell, Wales, UK).

The study was approved by the Institutional Review Board as designated by the Helsinki Declaration. All subjects gave their informed consent before their enrollment in the present study.

Magnetic resonance imaging

Subjects completed an MRI scan of the lower limb using a 0.5-T scanner (model Vectra 0.5, General Electric Corporation, Milwaukee, WI, USA) with an axial T1 weighted spin echo sequence. Axial views were acquired with 10-mm slice thickness and 50-mm interslice gap in 5 subjects and 10-mm in one subject. The lower limb lengths corresponding to the scan views are reported in Table 1. The area and volume of the skeletal muscle within each slice were calculated by a trained observer using the VECT image analysis software (Martel Inc., Montreal).

To obtain the discretized three-dimensional geometric model and tissue composition of the lower limb, as required by the BIA mathematical model, the MR images were scanned (Epson scanner Perfection mod. 1200Photo) with a resolution of 300 pixels per inch and then digitized. Each digitized image was then processed to identify the regions corresponding to the different tissues. Only three tissue types, namely bone, muscle, and adipose tissue were distinguished: cartilage and tendon were assigned to bone, vascular tissue to muscle, and skin to adipose tissue. Each tissue type was labeled by a different color. Each image was then subdivided into 22×22 square cells of 1-cm side, and cells were assigned to the prevailing tissue or to the external air.

In the final step, a text file was formed as a stack of discretized images. To have images at 1-cm intervals when the 50-mm interslice gap was used in the MRI scan, each of the available images was replicated 4 times (2 times the initial and the final image). The stack provided a three–dimensional model of lower limb geometry and tissue composition with a total, including the external air, of $22 \times 22 \times N$ cubic cells of 1 cm side, N depending on the length of subject's lower limb (N from 72 to 77, see Table 1).

Bioelectrical impedance analysis

Resistance and capacitive reactance were determined using a multifrequency BIA system (Human-IM DIP, DS-Medigroup, Milan, Italy), with a delivered current of 800 μA at a frequency of 50 kHz. The current-injection electrodes were positioned on the mid dorsum of the right hand, just proximal to metacarpal phalangeal joint line, and on the mid dorsum of the right foot, just proximal to metatarsal phalangeal joint line (3).

To determine the impedance profile along the lower limb, one of the voltage electrodes was positioned on the mid dorsum of the right wrist and kept fixed. The other electrode was positioned at various contiguous levels along the lower limb at 2.5 cm intervals, starting from the mid anterior right ankle up to the midline of the anterior surface of the right thigh at about the level of the inguinal crease. By subtracting the measured impedances from whole body impedance, we obtained the impedance profile along the lower limb, as would be measured between an electrode located at different levels along lower limb from the ankle to the hip and an electrode located at the ankle.

BIA mathematical model

As seen in the Appendix, the mathematical model for BIA consists of a set of equations of the form of Eq. 7A, one for each cell of the discretized three-dimensional model of lower limb. These equations associate an electrical network to the body region of interest, and the values of the admittances in the network depend on the electrical characteristics of the various tissues.

The electrical characteristics of tissues were obtained from literature data. For the conductivity (σ_{mz}) of skeletal muscle in the longitudinal direction, taken as the dominant direction

of muscle fibers in lower limb and corresponding to the z-axis in the model, we considered the values of 0.67 S/m and 0.85 S/m as reported in (6,7). The value of muscle conductivity in the transverse direction ($\sigma_{mx} = \sigma_{my}$) was set to 0.13 S/m as reported in (1). Both adipose tissue and bone were assumed to be isotropic tissues, with conductivity $\sigma_{at} = 0.064$ and $\sigma_b = 0.013$ S/m, respectively (1,4). The tissue permittivities were assumed to depend on the frequency of the applied current according to the following expressions (4):

$$\varepsilon_{mx} = \varepsilon_{my} = \varepsilon_o 10^{8.0 - 0.75 \log(1+f)}\,, \quad \varepsilon_{mz} = \varepsilon_o 10^{6.5 - 0.5 \log(1+f)}$$

$$\varepsilon_{at} = \varepsilon_o 10^{6.0 - 0.5 \log(1+f)}\,, \quad \varepsilon_b = \varepsilon_o 10^{4.0 - 0.33 \log(1+f)}$$

where $\varepsilon_o = 10^{-9}/(36\pi)$ F/m is the permittivity of free space. Conductivity and permittivity of external air were set equal to zero.

Concerning the externally applied current (the term I in equation $7A$) that simulates the current delivered to the body during BIA, we had to take into account that, in the present measurements of lower limb bioimpedance, the current-injecting electrodes were placed at locations that are far from the body region considered (i.e., in the ipsilateral hand and foot) to minimize the influence of current injection on the measurement of the potential. This condition was simulated by replicating the terminal cross-sections of the three-dimensional model of lower limb (one in the ankle and the other in the thigh), in order to create 10-cm extra-spaces below the ankle and, respectively, above the thigh. The external current was impressed in nodes of the electrical network located at the extreme of these extra spaces, so the region in which the distribution of electrical potential was calculated was at least 10 cm away from the points where the external current was applied.

Under the applied current, the network generated the distribution of the electrical potential in the body region considered, and thus allowed us to compute impedance values that were compared with data provided by BIA. The set of equations composing the model was solved by the technique of successive overrelaxation (4,10).

Estimation of muscle cross-sectional area and volume

A very simplified version of the model described in Appendix can provide estimates of muscle cross-sectional area and volume as detailed in the following. Because the longitudinal conductivity of muscle is much larger than all other conductivities, and the contribution of the reactive component of impedance is small at 50 kHz, we assume here that the z-directed current flowing in the lower limb during BIA is essentially carried by the resistive component of muscle, at least in lean subjects. Moreover we assume that, at locations remote from the current-injecting electrodes, the total z-directed current in a cross-section is equal to the total current, $\bar{I} = 800$ μA, delivered by the current-injecting electrodes. Thus, denoting the cross-sectional area by S and the muscle area by S_m (these areas change with the level z along the lower limb), and considering the component in the z–direction of the real part of the current density J (see the Appendix), we may write

$$\bar{I} \simeq \int_S J_z \, ds \simeq \int_{S_m} J_z \, ds \tag{1}$$

where ds is the element of cross-sectional area. Moreover, according to Eqs. $1A$-$4A$ of Appendix, we have

$$J_z = \sigma_{mz} \frac{\partial V}{\partial z}\,. \tag{2}$$

In a region far from the current-injecting electrodes, the electrical potential is likely to be approximately constant over the cross-section and thus V can be considered a function, $V(z)$, of z only. If the potential at the ankle ($z=0$) is set to zero, the quantity $V(z)/\bar{I}$ can be interpreted as the resistance between a point of the lower limb at distance z from the ankle and a point on the ankle itself. Denoting this resistance as $R(z)$, we have

$$R(z) = V(z)/\bar{I}\,. \tag{3}$$

Thus, Eqs. 1–3 give for any level z along the lower limb the equation

$$\sigma_{mz} S_m \frac{dR}{dz} \simeq 1\,, \tag{4}$$

and an estimate $\hat{S}_m(z)$ of the muscle cross-sectional area at the level z is obtained as:

$$\hat{S}_m(z) = \frac{1}{\sigma_{mz}} \frac{1}{dR/dz}\,. \tag{5}$$

To evaluate the derivative in Eq. 5, the resistance data obtained by BIA were fitted by a weighted sum of two gaussian cumulative functions plus a straight line, $\hat{R}(z)$, according to

$$\hat{R}(z) = c_1[F(z;0,\sigma_1) - 0.5] + c_2 F(z;\mu_2,\sigma_2) + c_3 z \tag{6}$$

where $F(z;\mu,\sigma)$ denotes the cumulative function of a gaussian with mean μ and SD σ and c_1-c_3 are constant coefficients (note that it should be $\hat{R}(0) \simeq 0$). The two cumulative gaussians represent the specific increase of resistance that is observed in the regions of the ankle and of the knee, respectively. The parameters c_1, c_2, c_3, σ_1, μ_2 and σ_2 of the fitting function were determined by minimization of a least-squares index. Then Eq. 5 was applied with $R(z) = \hat{R}(z)$ and $\sigma_{mz} = 0.85\,\mathrm{S/m}$. The integral over z of the estimated cross-sectional area of muscle provided the total muscle volume of the lower limb.

3. Results

Discretized model of lower limb

Although the discretization of MR images with cells of 1-cm side may seem approximate, the three-dimensional reconstruction of the geometry and tissue composition of the lower limb appeared in general to be rather accurate, at least as the content of muscle tissue is concerned. Figure 1 presents the cross-sectional area of the muscle, S_m, as computed on the original MR images in the 78 cross-sections of the lower limb of the subject in which the MRI scan was performed with 10-mm interslice gap. Moving from left to right ($z=0$ corresponds to the ankle), the regions corresponding to the ankle, the calf, the knee and the thigh are easily recognized. The total volume of muscle in the lower limb region considered, as measured from the original MR images, was equal to 5,751 cm^3.

The muscle areas given by the discretized three-dimensional model are also reported in Fig. 1. It is seen that the approximation becomes less accurate in the regions of the ankle and of the knee, where S_m is smaller. Considering all 78 cross-sections, the mean error on the area was 0.2 cm^2. The total volume of muscle in the discretized model was equal to 5,784 cm^3. Figure 1 shows also the less accurate approximation that was obtained for this subject when a reduced

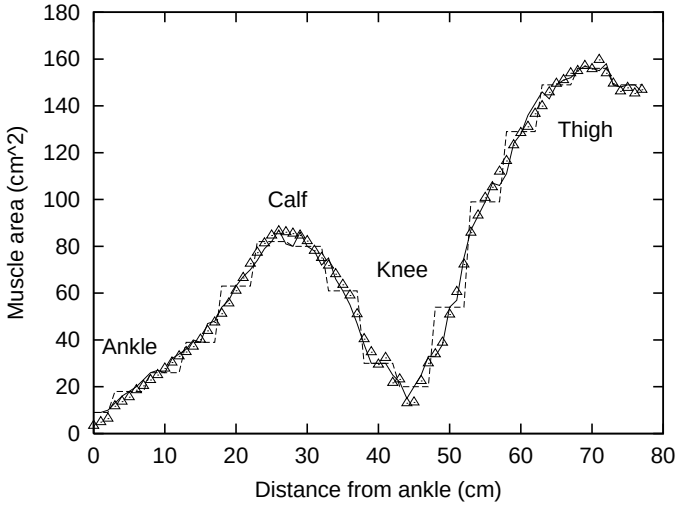

Fig. 1. Cross-sectional area of muscle along the lower limb of subject 1 from the ankle to the thigh: experimental data obtained from MRI (triangles), areas of muscle in the discretized three-dimensional model (continuous line), areas of muscle in the discretized model when cross-sections at 5-cm intervals are used (dashed line).

Table 1. *Lower limb muscle volume measured by MRI* (V_{MRI}) *and estimated from BIA* (V_{BIA}).

Subject[a]	Leg length[b] (cm)	V_{MRI} (cm^3)	V_{BIA} (cm^3)	Error[c]
1	77	5,751	5,394	6.21
2	76	4,197	4,493	−7.06
3	74	3,798	3,716	2.16
4	72	3,377	3,617	−7.10
5	72	3,396	3,829	−12.75
6	75	4,874	4,766	2.16

[a] Subjects 1–3 men, subjects 4–6 women

[b] Lower limb length corresponding to MR images

[c] Error: $100\times(V_{MRI}-V_{BIA})/V_{MRI}$.

number of cross-sections at 5-cm intervals was used. Although the errors on muscle areas are larger, the total volume of muscle given by the model in this case was equal to 5,945 cm^3, with an error smaller than 4% with respect to the original MRI data. Similar error values are likely to be found for the other subjects in which the discretized reconstruction of the lower limb was obtained from MR images taken at 5-cm intervals.

The volumes of muscle in the part of the lower limb considered in this study are reported in Table 1 (V_{MRI}) for the six subjects. For subject 1, for which MR images at 1 cm intervals were available, the volume measured on the original images is given.

Table 2. *Lower limb resistance and capacitive reactance measured by BIA (R_{BIA}, X_{BIA}) and given by the mathematical model (R_{MOD}, X_{MOD}).*

Subject[a]	R_{BIA} (Ω)	R_{MOD} (Ω)	X_{BIA} (Ω)	X_{MOD} (Ω)
1	238	253.2	33	24.7
2	237	247.9	38	27.1
3	250	274.2	31	29.5
4	261	261.7	32	27.1
5	246	268.1	32	30.6
6	250	262.6	31	28.3

[a] Subjects ordered as in Table 1.

Mathematical model of BIA and analysis of bioimpedance data

The distribution of the electrical potential provided by the BIA model shows that, in the proximity of the current-injecting electrodes, the potential varies considerably in the cross-section from the points closer to the electrode to the points far from it. This effect is markedly reduced in a cross-section at a distance of 10 cm. The variability of the potential V in the cross-section was quantified by computing the ratio $(V_{max} - V_{min})/V_{mean}$ in all of the cross-sections, including those of the added extra-spaces where the external current wass applied. In the cross-sections containing the electrodes, the above ratio was in the order of 10, whereas this ratio decreased to values lower than 0.3 in the cross-sections at least 10 cm away from the electrodes. However, in the region of the knee where the content of muscle tissue is lower, the ratio was larger and values up to 1.9 were achieved. When only the cells that form the border of a cross-section were considered, remarkable variations of the potential were still found in the region of the knee. Thus the location of the voltage electrode along the circumference of the limb at certain cross-sections is likely to affect the determination of the resistance.

The model provided also the currents that flow through the various tissues at each location within the lower limb. As expected, the currents flowing in the longitudinal direction (z-direction) in the muscle were markedly larger than the currents flowing in the other tissues. Far from the current-injecting electrodes, more than 90% of the z-directed current was carried by the muscle, except in the region of the knee where this percentage decreased to values around 70%. These results show that the assumptions leading to Eq. 5 may be considered substantially fulfilled.

The total resistance R_{BIA} and the capacitive reactance X_{BIA} of the part of lower limb considered, as measured by bioimpedance analysis, are reported in Table 2. The mean lower limb resistance was 243.7 Ω for men and 255.3 Ω for women. Reactances were in the range 31-38 Ω. These data appear to be adequately reproduced by the model (R_{MOD} and X_{MOD}, see Table 2) when the conductivity σ_{mz} of skeletal muscle in the longitudinal direction was set at 0.85 S/m (6). The model gave values of total resistance differing from the experimental data with relative errors smaller than 10%. The small contribution of the reactive component of the impedance at the frequency of 50 kHz was also shown by the model.

The profile of the resistance along the lower limb found by BIA in the subject in whom the MR images were available at 1-cm intervals is shown in Fig. 2. The experimental values

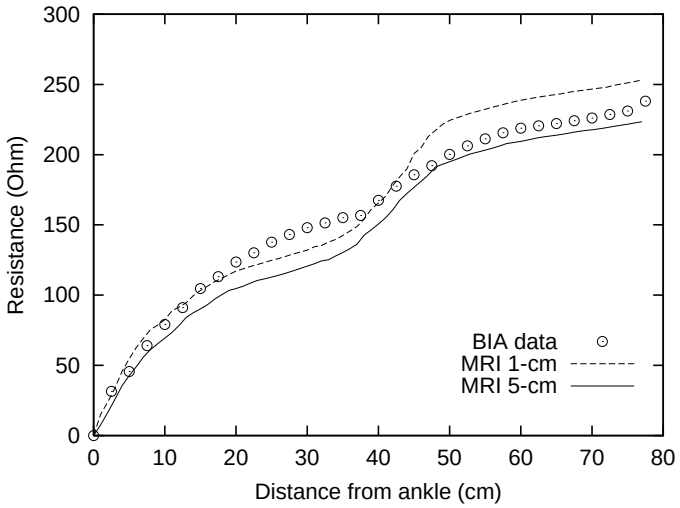

Fig. 2. Profile of resistance along the lower limb of subject 1 as given by BIA (circles); profile of resistance predicted by the model (dashed line); profile predicted by the model when only cross-sections at 5-cm intervals are considered (continuous line).

of the resistance are plotted at 2.5 cm intervals. The data show that the resistance increases more rapidly in the regions of the ankle and of the knee, where the content of low resistivity muscle tissue is smaller. Figure 2 reports also the profile of the resistance given by the model of Appendix, computed at each level z from the mean value of electrical potential over the cells that represent adipose tissue. The profile of the resistance obtained from the model when using the coarser discretization (MRI data at 5 cm intervals) is also reported in the figure and shows that the general pattern of the profile is still adequately reproduced by the BIA model when larger intervals are used for MR images. Figure 3 shows the experimental and predicted profiles for the lower limb of a woman.

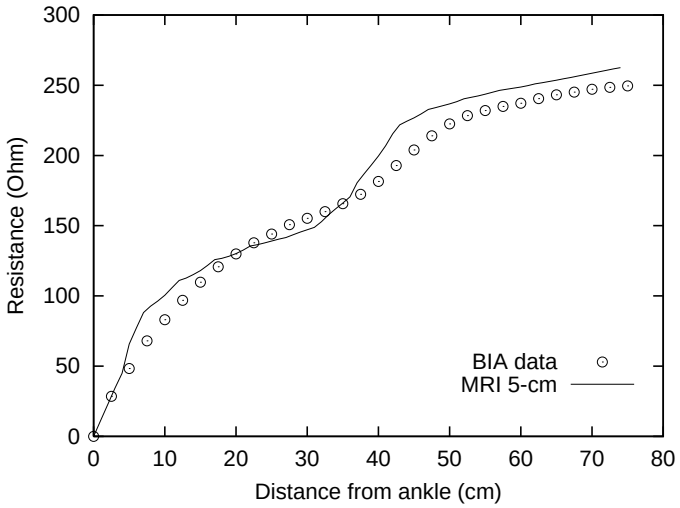

Fig. 3. Profile of resistance along the lower limb of subject 6 as given by BIA (circles); profile of resistance predicted by the model (continuous line).

Estimation of muscle cross-sectional area and volume

The estimation of the profile of muscle cross-sectional area along lower limb and of the muscle volume on the basis of Eqs. 5 and 6, using the experimental bioimpedance data, was found to be reasonably accurate for the estimated muscle volume. Table 1 reports the estimates of muscle volume (V_{BIA}) for all subjects. The mean±SD of the error with respect to MRI estimates was 6.2±3.9%. Mean±SD of the estimates of parameters of Eq. 6 (except μ_2 that depends on the length of the leg) are the following: c_1 =194.2±46.0 Ω, c_2 =73.2±7.6 Ω, c_3 =1.0±0.2 Ω/cm, σ_1 =10.4±1.7 cm, σ_2 =8.9±1.7 cm.

An example of the reconstruction of the profile of muscle cross-sectional area along the limb is shown in Fig. 4. The figure shows the experimental profile of resistance together with the fitted profile, $\hat{R}(z)$, and the muscle cross-sectional area obtained by Eq. 5, $\hat{S}_m(z)$, together with the areas given by MRI. Although the general pattern was reasonabe, large errors may by found at specific locations, such as the knee and the extreme sections of the thigh. These errors, however, did not cause a large effect on the estimate of total lower limb muscle volume.

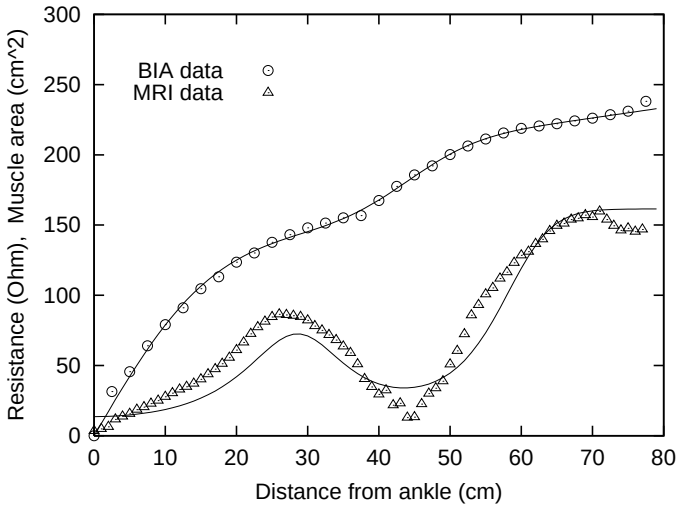

Fig. 4. Profile of resistance along the lower limb of subject 1 as given by BIA (circles) and fitted profile $\hat{R}(z)$ (continuous line). Muscle cross-sectional area along the lower limb of the same subject as obtained by MRI (triangles); profile of the muscle cross-sectional area as estimated by Eq. 5, $\hat{S}_m(z)$ (continuous line).

4. Discussion

In the past few years, a great deal of attention has focused on the evaluation of skeletal muscle mass, as a mean of assessing the nutritional status of individuals with various clinical conditions (8,13,14). For instance, there occurs loss of skeletal muscle tissue in patients following major accidents of the spinal cord and it is important and useful to monitor improvements in skeletal muscle mass and function with rehabilitation therapy (15,19,21).

The lower limb is well representative of whole body skeletal muscle mass in normal subjects with the exception of body builders or weight-lifters. The mathematical model of BIA here developed, that used the discretized reconstruction of lower limb geometry and tissue composition obtained by MRI, predicted the pattern of resistance along the lower limb as measured by

BIA. Because the model showed that the electrical current in lower limb is essentially carried by muscle, the pattern of resistance appears to be mainly dependent on the profile of muscle cross-sectional area along lower limb, and to contain thus the information needed for recovering the muscle volume from BIA data. The approach based on BIA could allow avoiding the more sophisticated and expensive technique based on MRI, at least in clinical practice and particularly when several measurements are required as in the present study.

Although some anatomical details is lost with MR images with cells of 1-cm side, the gross structure appeared to still be represented in the discretized three-dimensional model of the lower limb. Figure 1 shows that the profile of muscle area along the limb was rather accurately reproduced even when MR cross-sectional images at 5-cm intervals were available. Thus, the duration of the exposure during the MR scans can be reduced. We note, however, that with cells of 1-cm side the skin cannot be represented, even if its contribution to the flow of current across the limb is not negligible in the regions where the content of muscle and adipose tissue is reduced.

The model of BIA reproduced the general behavior of the impedance along the lower limb, as shown by Figures 2 and 3, at least when the value of the longitudinal conductivity of muscle (σ_{mz}) was set to a value of 0.85 S/m. It was found that the electrical potential along the border of a cross section of the limb can show marked changes, as also seen by BIA measurements (1). This effect is particularly remarkable in the proximity of the current-injecting electrodes and in the region of the knee, confirming that the location of the voltage electrodes may be critical in bioimpedance analysis.

As shown by Figures 2 and 3, the resistance profile given by the model did not follow precisely the experimental BIA data in the regions of the ankle and the knee, where the predicted resistance showed larger variations than those experimentally observed. A number of factors can cause these discrepancies: i) the predicted profile was obtained from the mean potential over the adipose tissue of the cross-section, whereas the experimental measurements were obtained by voltage electrodes at specific locations; ii) because of the discretization with cells of 1-cm side, anatomical structures such as ligaments, tendons and sinovial fluid were disregarded and these structures may present larger conductivities than those assumed in the model thus giving smaller increments in observed resistance; iii) the value of the longitudinal conductivity of muscle, σ_{mz}, which was assumed as a constant in the present model, may be partially dependent on interindividual variability as well as on the arrangement and orientation of the muscle fibers which is different in the thigh and in the calf (1).

Using the simplified model of Eqs. 5 and 6, the total muscle volume was estimated from the experimental BIA data with an acceptable error with respect to the reference value provided by MRI. The estimation of muscle cross-sectional area from the profile of resistance along the lower limb appears to be feasible, as shown by Figure 4. Because the measured potential can change when the voltage electrode is moved circumferentially at a given level of the limb, it is suggested that the measurement of the potential at more than a single point in a given cross-section (e.g., in both the anterior and the posterior aspects of the limb at the level of the knee) might provide a more accurate reconstruction of the muscle cross-sectional areas.

In conclusion, the mathematical model described in the present paper allows for predicting with good accuracy the volume of lower limb skeletal muscle mass by using BIA, thus representing a first step towards advancing BIA as a replacement for CT and MRI when evaluating the composition of lower limb.

Acknowledgements: The authors wish to thank Drs. A. Scarfone and P. Morini for technical assistance.

Appendix: Mathematical model of BIA

Under the quasi-static approximation, valid at the frequency $f = 50\,\mathrm{kHz}$ used in the present bioimpedance measurements, the electric field E (V/m) in the body region considered is related to the potential V (V) by the following equation

$$E = -\nabla V\,. \tag{1A}$$

Moreover, for the electric current density J (A/m^2) we can write the continuity equation

$$\nabla \cdot J = I \tag{2A}$$

where I (A/m^3) is the externally applied current per unit volume. Assuming harmonic fields, J is related to E by

$$J = \kappa E \tag{3A}$$

where κ (S/m) is the complex conductivity tensor given by

$$\kappa = \sigma + j2\pi f\varepsilon\,, \tag{4A}$$

σ being the conductivity and ε the permittivity of the media.

From Eqs. 1A-3A we obtain the following equation for the complex potential:

$$\nabla \cdot (\kappa \nabla V) = -I\,, \tag{5A}$$

to be solved in the region of interest with the appropriate boundary conditions (10). If the electric field is referred to Cartesian coordinates, all nondiagonal elements of the tensor $\kappa(x, y, z)$ are zero and $\kappa = \mathrm{diag}(\kappa_x, \kappa_y, \kappa_z)$. Thus, Eq. 5$A$ becomes

$$\frac{\partial}{\partial x}\left(\kappa_x \frac{\partial V}{\partial x}\right) + \frac{\partial}{\partial y}\left(\kappa_y \frac{\partial V}{\partial y}\right) + \frac{\partial}{\partial z}\left(\kappa_z \frac{\partial V}{\partial z}\right) = -I\,. \tag{6A}$$

The three components of the tensor κ at a given point (x, y, z) are possibly different because of tissue anisotropy, but the complex conductivity of a given tissue is assumed to be independent of the spatial position.

To solve Eq. 6A we used the finite difference method (4,20), the nodal points being taken coincident with the centers of the cells that form the three-dimensional model of the lower limb. The finite differences lead to the following equation (4):

$$V = \frac{1}{\sum_{i=1}^{6} Y_i}\left[\sum_{i=1}^{6} Y_i V_i + I\right] \tag{7A}$$

where V is the electrical potential in the node located at the center (x, y, z) of a cell, V_i are the potentials at the centers of the neighboring cells ($(x-\Delta x, y, z)$, $(x+\Delta x, y, z)$, and so on), Y_i are the complex admittances between the nodes, and I denotes the external current impressed at the node (x, y, z). It is $I \neq 0$ only at the nodes representing the current injecting electrodes.

The values of the admittances depend on the types of tissue associated to the various cells. For instance, the admittance Y_{x^+} between the points (x, y, z) and $(x+\Delta x, y, z)$ has the expression

$$Y_{x^+} = \frac{2\kappa_x(x,y,z)\kappa_x(x+\Delta x,y,z)}{\kappa_x(x,y,z)+\kappa_x(x+\Delta x,y,z)}\frac{\Delta y \Delta z}{\Delta x} \tag{8A}$$

and similarly for the other admittances. The impedances to be compared with BIA data were computed from the mean value of the electrical potential over the cells that represent adipose tissue at a given level z along the lower limb.

References

1. Aaron, R., M. Huang, and C.A Shiffman. Anisotropy of human muscle via non-invasive impedance measurements. *Phys. Med. Biol.* 42: 1245-1262, 1997.
2. Baumgartner, R.N., R. Ross, and S.B. Heymsfield. Does adipose tissue influence bioelectric impedance in obese men and women? *J. Appl. Physiol.* 84: 257-262, 1998.
3. Bioelectrical impedance analysis in body composition measurement: National Institutes of Health Technology Assessment Conference Statement. *Am. J. Clin. Nutr.* 64: 524S-532S, 1996.
4. D'Inzeo, G., C. Giacomozzi, and S. Pisa. Analysis of the stimulation of a nerve fiber surrounded by an inhomogeneous, anisotropic, and dispersive tissue. *Appl. Comput. Electromagnet. Soc. J.* 7: 179-190, 1992.
5. Ellis, K.J., S.J. Bell, G.M. Chertow, W.C. Chumlea, T.A. Knox, D.P. Kother, H.C. Lukaski, and D.A Shoeller. Bioelectrical impedance methods in clinical research: a follow-up to the NIH Technology Assessment Conference. *Nutrition* 15: 874-880, 1999.
6. Fuller, N.J., M.B. Sawuer, M.A. Laskey, P. Paxton, and M. Elia. Prediction of body composition in elderly men over 75 years of age. *Ann. Hum. Physiol.* 23: 127-147, 1996.
7. Fuller, N.J., C.R. Hardingham, M. Graves, N. Screaton, A.K. Dixon, L.C. Ward, and M. Elia. Predicting composition of leg sections with anthropometry and bioelectrical impedence analysis, using magnetic resonance imaging as reference. *Clin. Sci.* 96: 647-657, 1999.
8. Gallagher, D., M. Visser, R.E. DeMeersman, D. Sepulveda, R.N. Baumgartner, R.N. Pierson, Jr., and T. Harris. Appendicular skeletal muscle mass: effects of age, gender, and ethnicity. *J. Appl. Physiol.* 83: 229-239, 1997.
9. Goodpaster, B.H., F.L. Thaete, and D.E. Kelley. Composition of skeletal muscle evaluated with computed tomography. *Ann. N.Y. Acad. Sci.* 904: 18-24, 2000.
10. Heringa, A., D.F. Stegeman, G.J.H. Uijen, and J.P.C de Weerd. Solution methods of electrical field problems in physiology. *IEEE Trans. Biomed. Eng.* 29: 34-42, 1982.
11. Heymsfield, S.B., Z. Wang, M. Visser, D. Gallagher, and R.N. Pierson, Jr. Techniques used in the measurement of body composition: an overview with emphasis on bioelectrical impedance analysis. *Am. J. Clin. Nutr.* 64: 478S-484S, 1996.
12. Heymsfield, S.B., Z.M. Wang, R.N. Baumgartner, and R. Ross. Human body composition: advances in models and methods. *Ann. Rev. Nutr.* 17: 527-558, 1997.
13. Janssen, I., S.B. Heymsfield, Z.M. Wang, and R. Ross. Skeletal muscle mass and distribution in 468 men and women aged 18-88 yr. *J. Appl. Physiol.* 89: 81-88, 2000.

14. Janssen, I., S.B. Heymsfield, R.N. Baumgartner, and R. Ross. Estimation of skeletal muscle mass by bioelectrical impedance analysis. *J. Appl. Physiol.* 89: 465-471, 2000.

15. Mooney, V., J. Gulick, M. Perlman, D. Levy, R. Pezos, S. Leggett, and D. Resnik. Relationships between myoelectric activity, strength, and MRI of lumbar extensor muscles in back pain patients and normal subjects. *J. Spinal Disord.* 10: 348-356, 1997.

16. Organ, L.W., G.B. Bradham, D.T. Gore, and S.L. Lozier. Segmental bioelectrical impedance analysis: theory and application of a new technique. *J. Appl. Physiol.* 77: 98-112, 1994.

17. Pietrobelli, A., P. Morini, N. Battistini, G. Chiumello, C. Nuñez, and S.B. Heymsfield. Appendicular skeletal muscle mass: prediction from multiple frequency segmental bioimpedance analysis. *Eur. J. Clin. Nutr.* 52: 507-511, 1998.

18. Ross, R., B. Goodpaster, D. Kelley, and F. Boada. Magnetic resonance imaging in human body composition research. From quantitative to qualitative measurement. *Ann. N.Y. Acad. Sci.* 904: 12-17, 2000.

19. Scremin, A.N., L. Kurta, A. Gentili, B. Weiseman, K. Perell, and O.U. Soremin. Increasing muscle mass in spinal cord injured persons with a functional electrical stimulation exercise program. *Arch. Phys. Med. Rehabil.* 80: 1531-1536, 1999.

20. Sowiński, M.J., and P.M. van den Berg. A three-dimensional iterative scheme for an electromagnetic capacitive applicator. *IEEE Trans. Biomed. Eng.* 37: 975-986, 1990.

21. Visser, M., T.B. Harris, K.M. Fox, W. Hawkes, J.R. Hebel, J.Y. Yahiro, R. Michael, S.I. Zimmermann, and J. Magaziner. Change in muscle mass and muscle strength after a hip fracture: relationship to mobility recovery. *J. Gerontol. A. Biol. Sci. Med. Sci.* 55: M434-M440, 2000.